

Electronic Modulation of Hyperpolarizable (Porphinato)zinc(II) Chromophores Featuring Ethynylphenyl-, Ethynylthiophenyl-, Ethynylthiazolyl-, and Ethynylbenzothiazolyl-Based Electron-Donating and -Accepting Moieties

Tian-Gao Zhang,[†] Yuxia Zhao,[§] Kai Song,[‡] Inge Asselberghs,[‡] André Persoons,[‡] Koen Clays,^{*,‡} and Michael J. Therien^{*,†}

Center for Research on Molecular Electronics and Photonics, University of Leuven, B-3001 Leuven, Belgium, Technical Institute of Physics and Chemistry, Chinese Academy of Sciences, Beijing 100080, China, and Department of Chemistry, University of Pennsylvania, Philadelphia, Pennsylvania 19104-6323

Received May 23, 2006

A series of conjugated (porphinato)zinc(II)-based chromophores structurally related to [5-(4-dimethylaminophenylethynyl)-15-(5-nitrothienyl-2-ethynyl)-10,20-bis(3,5-bis(3,3-dimethyl-1-butoxy)phenyl)porphinato]zinc(II) were synthesized using metal-catalyzed cross-coupling reactions involving [5-bromo-15-triisopropylsilylethynyl-10,20-diarylporphinato]zinc(II), [5-bromo-15-(4-dimethylaminophenylethynyl)-10,20-diarylporphinato]zinc(II), [5-(4-dimethylaminophenylethynyl)-15-ethynyl-10,20-diarylporphinato]zinc(II), and [5-(4-nitrophenylethynyl)-15-ethynyl-10,20-diarylporphinato]zinc(II), along with appropriately functionalized aryl, thienyl (or thiophenyl), thiazolyl, benzothiazolyl, and carbazolyl precursors. The linear and nonlinear optical properties of these asymmetrically 5,15-substituted-(10,20-diarylporphinato)zinc(II) chromophores that bear either 2-(9H-carbazol-9-yl)-thiophen-5-yl-ethynyl, 4-dimethylaminophenylethynyl, or 2-(*N,N*-diphenylamino)thiophen-5-yl-ethynyl electron-releasing groups and an electron-withdrawing group selected from 2-formyl-thiophen-5-yl-ethynyl, 2-(2,2-dicyanovinyl)-thiophen-5-yl-ethynyl, 4-nitrophenylethynyl, 6-nitrobenzothiazol-2-yl-ethynyl, or 5-nitrothiazol-2-yl-ethynyl are reported. The dynamic hyperpolarizabilities of these compounds were determined from hyper-Rayleigh light scattering measurements carried out at a fundamental incident irradiation wavelength (λ_{inc}) of 1300 nm; these measured β_{1300} values ranged from 690 \rightarrow 1400 $\times 10^{-30}$ esu. These data (i) show that these neutral dipolar molecules express substantial β_{1300} values, (ii) highlight that reductions in the magnitude of the aromatic stabilization energy of (porphinato)metal-pendant arylethynyl groups have a significant impact upon the magnitude of the molecular hyperpolarizability, and (iii) provide insights into advantageous design modifications for closely related structures having potential utility in long-wavelength electrooptic applications.

Introduction

Thiophene and thiazole rings, among five-membered heteroaromatics, have received appreciable attention as highly polarizable π -bridges for nonlinear optical (NLO) materials,^{1–12} and media for electron- and energy-transfer reactions.^{13–18}

The low aromatic stabilization energy (ASE)^{1,19,20} coupled with the electron-rich nature of these species relative to six-membered aromatic carbocyclics²¹ drive the utility of thiophene- and thiazole-containing structures in electrooptic materials.

Likewise, porphyrin-based building blocks have also figured prominently in the range of unusually polarizable

* To whom correspondence should be addressed. E-mail: koen.clays@fys.kuleuven.be (K.C.); therien@sas.upenn.edu (M.J.T.).

[‡] University of Leuven.

[§] Chinese Academy of Sciences.

[†] University of Pennsylvania.

(1) Breitung, E. M.; Shu, C.-F.; McMahon, R. J. *J. Am. Chem. Soc.* **2000**, *122*, 1154–1160.

(2) Raimundo, J.-M.; Blanchard, P.; Gallego-Planas, N.; Mercier, N.; Ledoux-Rak, I.; Hierle, R.; Roncali, J. *J. Org. Chem.* **2002**, *67*, 205–218.

(3) Miller, R. D.; Lee, V. Y.; Moylan, C. R. *Chem. Mater.* **1994**, *6*, 1023–1032.

and hyperpolarizable structures.^{22–32} The coupling of thiophene rings with porphyrinic units has been exploited in the development of NLO chromophores that possess substantial molecular hyperpolarizabilities at a fundamental incident irradiation wavelength (λ_{inc}) of 1300 nm;^{29,33} interestingly, the linear and nonlinear optical properties of this series of electronically asymmetric porphyrin-(oligo)thiophene chromophores challenge the classic concept of the nonlinearity/transparency tradeoff in charge-transfer chromophores.²⁹

We report herein a complimentary set of conjugated (porphinato)zinc(II)-based chromophores structurally related to [5-(4-dimethylaminophenylethynyl)-15-(5-nitrothienyl)-2-

ethynyl)-10,20-bis(3,5-bis(3,3-dimethyl-1-butyloxy)phenyl)porphinato]zinc(II)²⁹ that features ethynylphenyl-, ethynylthiophenyl-, ethynylthiazolyl-, and ethynylbenzothiazolyl-based electron-donating and -accepting moieties. These species were synthesized via metal-catalyzed cross-coupling reactions involving [5-bromo-15-triisopropylsilylethynyl-10,20-diarylporphinato]zinc(II), [5-bromo-15-(4-dimethylaminophenylethynyl)-10,20-diarylporphinato]zinc(II), [5-(4-dimethylaminophenylethynyl)-15-ethynyl-10,20-diarylporphinato]zinc(II), and [5-(4-nitrophenylethynyl)-15-ethynyl-10,20-diarylporphinato]zinc(II), along with appropriately functionalized aryl, thienyl, thiazolyl, benzothiazolyl, and carbazolyl precursors. We describe the linear spectroscopic properties and determine the dynamic hyperpolarizabilities (β_{λ} values) measured via hyper-Rayleigh light scattering (HRS) for 1300 nm incident irradiation. These data show that these neutral dipolar molecules express substantial β_{1300} values and provide insights into design modifications for closely related structures with potential utility in long-wavelength electrooptic applications.

Experimental Section

Materials. Inert atmosphere manipulations were carried out under nitrogen prepurified by passage through an O₂ scrubbing tower (Schweizerhall R3-11 catalyst) and a drying tower (Linde 3-Å molecular sieves). Air-sensitive solids were handled in a Braun 150-M glovebox. Standard Schlenk techniques were employed to manipulate oxygen- and moisture-sensitive chemicals. Tetrahydrofuran (Fisher Scientific, HPLC grade) was distilled from potassium/benzophenone, while diethylamine and triethylamine were distilled from CaH₂; DMF (anhydrous), toluene (anhydrous), 1,2-dichloroethane (anhydrous), *o*-xylene (anhydrous), diisopropylamine (redistilled, 99.5%), and *N,N*-diisopropylethylamine (redistilled, 99.5%) were used as received from Aldrich. Pd₂(dba)₃, Pd(PPh₃)₄, CuI, AsPh₃, P(*t*-Bu)₃, *n*-BuLi, and NaO(*t*-Bu) were obtained from either Aldrich or Strem. *n*-Tetrabutylammonium fluoride (TBAF) (1.0 M in THF) was obtained from Aldrich, while trimethylsilylacetylene was obtained from GFS Chemicals. Alumina (neutral, grade I) and iodine were obtained from Fisher. Diphenylamine, 9*H*-carbazole, 2-iodothiophene, 2-bromothiazole, 2-amino-6-nitrobenzothiazole, isomaylnitrite, diiodomethane, 5-(trimethylsilylethynyl)-thiophene-2-carbaldehyde, and malononitrile were purchased from Aldrich. 2-Ethynyl-5-nitrothiophene was synthesized via established methods.^{34–36} 5-(Trimethylsilylethynyl)-thiophene-2-carbaldehyde was synthesized following a literature method.³⁷ The syntheses of 5,15-bis(3,5-bis(3,3-dimethyl-1-butyloxy)phenyl)porphyrin, [5-bromo-10,20-bis(3,5-bis(3,3-dimethyl-1-butyloxy)phenyl)porphinato]zinc(II), [5,15-dibromo-10,20-bis(3,5-bis(3,3-dimethyl-1-butyloxy)phenyl)porphinato]zinc(II), [5-bromo-15-triisopropylsilylethynyl-10,20-diarylporphinato]zinc(II) (**porphyrin 1**), [5-(4-dimethylaminophenylethynyl)-15-bromo-10,20-bis(3,5-bis(3,3-dimethyl-1-butyloxy)phenyl)porphinato]zinc(II) (**porphyrin 2**), [5-(4-dimethylaminophenylethynyl)-15-ethynyl-10,20-diarylporphinato]zinc(II) (**por-**

- (4) Davey, M. H.; Lee, V. Y.; Wu, L.-M.; Moylan, C. R.; Volksen, W.; Knoesen, A.; Miller, R. D.; Marks, T. J. *J. Chem. Mater.* **2000**, *12*, 1679–1693.
- (5) Cai, C.; Liakatas, I.; Wong, M.-S.; Bosch, M.; Bosshard, C.; Gunter, P.; Concilio, S.; Tirelli, N.; Suter, U. W. *Org. Lett.* **1999**, *1*, 1847–1849.
- (6) Wang, Y.-K.; Shu, C.-F.; Breitung, E. M.; McMahon, R. J. *J. Mater. Chem.* **1999**, *9*, 1449–1452.
- (7) Dirk, C. W.; Katz, H. E.; Schilling, M. L.; King, L. A. *J. Chem. Mater.* **1990**, *2*, 700–705.
- (8) Casado, J.; Pappenfus, T. M.; Miller, L. L.; Mann, K. R.; Orti, E.; Viruela, P. M.; Pou-Amerigo, R.; Hernandez, V.; Lopez Navarrete, J. T. *J. Am. Chem. Soc.* **2003**, *125*, 2524–2534.
- (9) Kim, O.-K.; Fort, A.; Barzoukas, M.; Blanchard-Desce, M.; Lehn, J.-M. *J. Mater. Chem.* **1999**, *9*, 2227–2232.
- (10) Rao, V. P.; Jen, A. K. Y.; Wong, K. Y.; Drost, K. J. *Tetrahedron Lett.* **1993**, *34*, 1747–1750.
- (11) Bedworth, P. V.; Cai, Y.; Jen, A.; Marder, S. R. *J. Org. Chem.* **1996**, *61*, 2242–2246.
- (12) Steybe, F.; Effenberger, F.; Gubler, U.; Bosshard, C.; Gunter, P. *Tetrahedron* **1998**, *54*, 8469–8480.
- (13) Odobel, F.; Suresh, S.; Blart, E.; Nicolas, Y.; Quintard, J.-P.; Janvier, P.; Le Questel, J.-Y.; Illien, B.; Rondeau, D.; Richomme, P.; Haupl, T.; Wallin, S.; Hammarstrom, L. *Chem.—Eur. J.* **2002**, *8*, 3027–3046.
- (14) Effenberger, F.; Wuerthner, F.; Steybe, F. *J. Org. Chem.* **1995**, *60*, 2082–2091.
- (15) Wuerthner, F.; Vollmer, M. S.; Effenberger, F.; Emele, P.; Meyer, D. U.; Port, H.; Wolf, H. C. *J. Am. Chem. Soc.* **1995**, *117*, 8090–8099.
- (16) Vollmer, M. S.; Wurthner, F.; Effenberger, F.; Emele, P.; Meyer, D. U.; Stumpfig, T.; Port, H.; Wolf, H. C. *Chem.—Eur. J.* **1998**, *4*, 260–269.
- (17) Vollmer, M. S.; Effenberger, F.; Stumpfig, T.; Hartschuh, A.; Port, H.; Wolf, H. C. *J. Org. Chem.* **1998**, *63*, 5080–5087.
- (18) Ikemoto, J.; Takimiya, K.; Aso, Y.; Otsubo, T.; Fujitsuka, M.; Ito, O. *Org. Lett.* **2002**, *4*, 309–311.
- (19) Cook, M. J.; Katritzky, A. R.; Linda, P. In *Adv. Heterocycl. Chem.*; Katritzky, A. R., Boulton, A. J., Eds.; Academic Press: New York, 1974; Vol. 17, pp 255–356.
- (20) Wheland, G. W. *Resonance in Organic Chemistry*; Wiley: New York, 1955.
- (21) Smith, M. B.; March, J. *March's Advanced Organic Chemistry: Reactions, Mechanisms, and Structure*, 5th ed.; Wiley: New York, 2001.
- (22) Lin, V. S.-Y.; DiMagno, S. G.; Therien, M. J. *Science* **1994**, *264*, 1105–1111.
- (23) LeCours, S. M.; Guan, H.-W.; DiMagno, S. G.; Wang, C. H.; Therien, M. J. *J. Am. Chem. Soc.* **1996**, *118*, 1497–1503.
- (24) LeCours, S. M.; DiMagno, S. G.; Therien, M. J. *J. Am. Chem. Soc.* **1996**, *118*, 11854–11864.
- (25) Susumu, K.; Therien, M. J. *J. Am. Chem. Soc.* **2002**, *124*, 8550–8552.
- (26) Uyeda, H. T.; Zhao, Y.; Wostyn, K.; Asselberghs, I.; Clays, K.; Persoons, A.; Therien, M. J. *J. Am. Chem. Soc.* **2002**, *124*, 13806–13813.
- (27) Angiolillo, P. J.; Uyeda, H. T.; Duncan, T. V.; Therien, M. J. *J. Phys. Chem. B.* **2004**, *108*, 11893–11903.
- (28) Duncan, T. V.; Rubtsov, I. V.; Uyeda, H. T.; Therien, M. J. *J. Am. Chem. Soc.* **2004**, *126*, 9474–9475.
- (29) Zhang, T.-G.; Zhao, Y.; Asselberghs, I.; Persoons, A.; Clays, K.; Therien, M. J. *J. Am. Chem. Soc.* **2005**, *127*, 9710–9720.
- (30) Susumu, K.; Duncan, T. V.; Therien, M. J. *J. Am. Chem. Soc.* **2005**, *127*, 5186–5195.
- (31) Yeung, M.; Ng, A. C. H.; Drew, M. G. B.; Vorpagel, E.; Breitung, E. M.; McMahon, R. J.; Ng, D. K. P. *J. Org. Chem.* **1998**, *63*, 7143–7150.

(32) Anderson, H. L. *Chem. Commun.* **1999**, 2323–2330.

(33) Zhang, T.-G. Ph.D. Thesis, University of Pennsylvania, 2003.

(34) Mueller, T. J. J.; Robert, J. P.; Schmaelzlin, E.; Braeuchle, C.; Meerholz, K. *Org. Lett.* **2000**, *2*, 2419–2422.

(35) Xia, A.; Selegue, J. P. *Inorg. Chim. Acta* **2002**, *334*, 219–224.

(36) Vegh, D.; Kovac, J.; Dandarova, M. *Tetrahedron Lett.* **1980**, *21*, 969–970.

(37) Wu, I.-Y.; Lin, J. T.; Luo, J.; Li, C.-S.; Tsai, C.; Wen, Y. S.; Hsu, C.-C.; Yeh, F.-F.; Liou, S. *Organometallics* **1998**, *17*, 2188–2198.

phyrin 3), and [5-ethynyl-15-(4-nitrophenylethynyl)-10,20-diarylporphinato]zinc(II) (**porphyrin 4**) have been reported previously.^{23,25,26,29,38} The synthesis and electrooptic properties of the nonlinear optical chromophore [5-(4-dimethylaminophenylethynyl)-15-(5-nitrothienyl-2-ethynyl)-10,20-bis(3,5-bis(3,3-dimethyl-1-butyloxy)phenyl)porphinato]zinc(II) (**compound 1**) have been described recently.²⁹

¹H NMR spectra were recorded on either 250 MHz Bruker AC-250 or 360 MHz Bruker AM-360 spectrometers. All chemical shifts for ¹H NMR spectra are relative to that of TMS. All *J* values are reported in Hertz; the number of attached protons is found in parentheses following the chemical shift value. Chromatographic purification (silica gel 60, 230–400 mesh, EM Scientific; Bio-Beads S-X1, Bio-Rad Laboratories) of all newly synthesized compounds was accomplished on the benchtop. MALDI-TOF mass spectroscopic data were obtained with either an Applied Biosystems Perceptive Voyager-DE instrument in the Laboratories of Dr. Virgil Percec (Department of Chemistry, University of Pennsylvania) or a PerSpective BioSystems Voyager-DE instrument in the Laboratories of Dr. William DeGrado (Department of Biochemistry and Biophysics, University of Pennsylvania School of Medicine). Samples were prepared as micromolar solutions in THF, and either dithranol (Aldrich) or α -cyano-4-hydroxy cinnamic acid (α -CHCA) was utilized as the matrix. FAB data was obtained at the Drexel Mass Spectrometry facility. Electrospray ionization (ESI-MS) and chemical ionization (CI-MS) data were obtained in the University of Pennsylvania Chemistry Mass Spectrometry Facility.

Instrumentation. Electronic spectra were recorded on an OLIS UV/vis/near-IR spectrophotometry system that is based on the optics of a Cary 14 spectrophotometer. Emission spectra were recorded on a SPEX Fluorolog luminescence spectrophotometer that utilized a T-channel configuration with a red-sensitive R2658 Hamamatsu PMT and liquid-nitrogen-cooled InGaAs detector; these spectra were corrected using the spectral output of a calibrated light source supplied by the National Bureau of Standards. Time-correlated single photon counting (TCSPC) spectroscopic measurements were performed at the Regional Laser and Biotechnology Laboratory (RLBL) at the University of Pennsylvania using an instrument described previously;³⁹ these data were analyzed using Lifetime (RLBL) and Globals Unlimited (LFD, University of Illinois) Programs.

HRS Measurements. Femtosecond HRS experiments were performed at 1300 nm.⁴⁰ Disperse red 1 (DR1, $\beta_{1300} = 54 \times 10^{-30}$ esu in CHCl₃) was utilized as a reference dipolar chromophore. Standard local field correction factors were applied [$(n_D^2 + 2)/3$]³, where *n* is the refractive index of the solvent at the sodium D line], to correct for the solvent dependence of the hyperpolarizability of the external reference. Note that these experiments were performed at low chromophore concentrations ($<4 \times 10^{-5}$ M⁻¹); the linearity of the HRS signal as a function of chromophore concentration confirmed that no significant self-absorption of the second harmonic generation (SHG) signal occurred in these experiments. HRS signals measured for the dipolar 5,15-disubstituted-(10,20-diarylporphinato)zinc(II) chromophores were analyzed as resulting from a single major hyperpolarizability tensor component, i.e., the diagonal component β_{zzz} ⁴¹ along the molecular *z* axis, which corresponds in the molecular reference frame to the axis of highest conjugation.

Synthesis of Nonlinear Optical Chromophores. Synthetic details and analytical data for all precursor compounds are described in the Supporting Information.

[5-(4-Dimethylaminophenylethynyl)-15-(2-formylthiophen-5-yl-ethynyl)-10,20-bis(3,5-bis(3,3-dimethyl-1-butyloxy)phenyl)porphinato]zinc(II) (Compound 2). Porphyrin 2 (12.8 mg, 11.1 μ mol), 5-ethynylthiophene-2-carbaldehyde (12.2 mg, 89.9 μ mol), Pd(PPh₃)₄ (38 mg, 32.8 μ mol), CuI (12 mg, 63.0 μ mol), THF (20 mL), and triethylamine (5 mL) were placed into a Schlenk tube, and the reaction mixture was stirred at 55 °C for 18 h. The reaction mixture was monitored via electron absorption spectroscopy. After the reaction mixture was filtered and evaporated, the green residue was chromatographed sequentially over silica gel (3:1 hexanes/THF), size-exclusion media (BioBeads S-X1, BioRad, THF), and silica gel (CHCl₃). A green solid was obtained after evaporation of solvent. Yield: 12 mg (92%, based on 12.8 mg of the porphyrinic starting material). ¹H NMR (CDCl₃/TMS/pyridine-*d*₅): δ 9.93 (s, 1H, CHO), 9.69 (d, 2H, β , *J* = 4.58), 9.54 (d, 2H, β , *J* = 4.49), 8.97 (d, 2H, β , *J* = 4.44), 8.92 (d, 2H, β , *J* = 4.44), 7.88 (d, 2H, Ar, *J* = 8.71), 7.77 (d, 1H, thienyl, *J* = 3.96), 7.62 (d, 1H, thienyl, *J* = 3.91), 7.32 (d, 4H, Ar, *J* = 2.25), 6.87 (m, 4 H, Ar), 4.21 (t, 8 H, OCH₂CH₂), 3.10 (s, 6H, NMe₂), 1.85 (t, 8H, OCH₂CH₂), 1.01 (s, 36 H, *tert*-butyl). Vis ($\lambda_{\max}(\log \epsilon)$; THF): 461 (5.26), 676 (4.74). Fluorescence emission (THF): 696 nm. MALDI-TOF: 1202.5, calcd for C₇₃H₇₉N₅O₅SZn: 1201.5.

[5-(4-Dimethylaminophenylethynyl)-15-(2-(2,2-dicyanovinyl)-thiophen-5-yl-ethynyl)-10,20-bis(3,5-bis(3,3-dimethyl-1-butyloxy)phenyl)porphinato]zinc(II) (Compound 3). Compound 2 (147 mg, 122 μ mol), and malononitrile (180 mg, 2.72 mmol) were placed in a 100 mL Schlenk tube and dried under vacuum. Alumina (neutral activity I, 1.04 g) and THF (30 mL) were added; after three freeze–pump–thaw cycles, the mixture was stirred at room temperature (RT) for 9.5 h. The mixture was then filtered and evaporated to give a brownish-green residue which was sequentially flash-chromatographed over silica gel (CHCl₃), Bio-Beads SX-1 (THF), and silica gel (CHCl₃), to give the product, isolated as a brown-green solid. Yield: 105 mg (69%, based on 147 mg of the porphyrinic starting material). ¹H NMR (pyridine-*d*₅): δ 10.14 (d, 2 H, β , *J* = 4.25), 9.87 (d, 2 H, β , *J* = 4.44), 9.35 (d, 4 H, β , *J* = 4.54), 8.45 (s, 1 H, vinylic), 8.18 (d, 2 H, phenyl, *J* = 8.57), 7.82 (d, 1 H, thienyl, *J* = 4.16), 7.80 (d, 4 H, phenyl, *J* = 1.72), 7.76 (d, 1 H, thienyl, *J* = 3.78), 7.39 (m, 2 H, Ar), 6.94 (d, 2 H, phenyl, *J* = 8.86), 4.36 (t, 8 H, OCH₂CH₂, *J* = 7.07, 7.01), 2.90 (s, 6 H, NMe₂), 1.91 (t, 8 H, OCH₂CH₂, *J* = 6.95, 7.14), 0.98 (s, 36 H, *tert*-butyl). Vis ($\lambda_{\max}(\log \epsilon)$; THF): 469 (4.69), 698 (4.41). Fluorescence emission (THF): 759 nm. MALDI-TOF: 1250.0 (M⁺); ESI-MS: 1249.5; calcd for C₇₆H₇₉N₇O₄SZn: 1249.5.

[5-(4-Dimethylaminophenylethynyl)-15-(6-nitrobenzothiazol-2-yl-ethynyl)-10,20-bis(3,5-bis(3,3-dimethyl-1-butyloxy)phenyl)porphinato]zinc(II) (Compound 4). Porphyrin 3 (113 mg, 0.103 mmol), 2-iodo-6-nitrobenzothiazole (331 mg, 1.08 mmol), Pd(PPh₃)₄ (122 mg, 0.105 mmol), CuI (31 mg, 0.163 mmol), THF (20 mL), and (*i*-Pr)₂NEt (1.6 mL) were placed in a 100 mL Schlenk tube and heated at 60 °C for 19 h. After cooling to RT, the mixture was poured into deionized water, extracted with methylene chloride,

(41) Note: In the NLO community, β_{zzz} denotes a first hyperpolarizability tensor component along the dipolar molecular *z* axis for charge transfer, while β_{xxx} refers to one of the four nonzero hyperpolarizability tensor components for a *D*_{3h}-symmetric octopolar molecule in the *xy* plane, the *z* axis again being the unique molecular axis perpendicular to this plane. With respect to the previous body of literature describing the electronic transitions of electronically asymmetric [5,15-bis(aryl-ethynyl)porphinato]metal compounds, the axis of longest conjugation is denoted as *x*.

(38) DiMaggio, S. G.; Lin, V. S.-Y.; Therien, M. J. *J. Org. Chem.* **1993**, *58*, 5983–5993.

(39) Holtom, G. R. *SPIE* **1990**, *1204*, 2–12.

(40) Olbrechts, G.; Wostyn, K.; Clays, K.; Persoons, A. *Opt. Lett.* **1999**, *24*, 403–405.

dried over Na₂SO₄, filtered, and evaporated. The green residue was chromatographed sequentially over silica gel, Bio-Beads SX-1 (THF), and silica gel (19:1 CHCl₃/THF). Yield: 101 mg (77% based on 113 mg of the porphyrinic starting material). ¹H NMR (CDCl₃/TMS/1-drop-pyridine-*d*₅): δ 9.68 (d, 2 H, β, *J* = 4.43), 9.59 (d, 2 H, β, *J* = 4.77), 9.00 (d, 2 H, β, *J* = 4.49), 8.91 (d, 2 H, β, *J* = 4.60), 8.65 (d, 1 H, H7 of 6-nitrobenzothiazolyl acceptor, *J* = 2.11), 8.25 (dd, 1 H, H5 of 6-nitrobenzothiazolyl acceptor, *J* = 2.19, 6.83, 2.14), 7.98 (d, 1 H, H4 of 6-nitrobenzothiazolyl acceptor, *J* = 8.97), 7.86 (d, 2 H, Ar, *J* = 8.82), 7.35 (d, 4 H, Ar, *J* = 2.10), 6.90 (t, 2 H, Ar, *J* = 2.25, 2.24), 6.82 (d, 2 H, Ar, *J* = 8.86), 4.23 (t, 8 H, OCH₂ CH₂), 3.08 (s, 6 H, NMe₂), 1.85 (t, 8 H, OCH₂ CH₂), 1.02 (s, 36 H, *tert*-butyl). Vis (λ_{max}(log ε); THF): 465 (5.25), 686 (4.87). Fluorescence emission (THF): 716 nm. ESI-MS: 1269.56 (M⁺), calcd for C₇₅H₇₉N₇O₆SZn: 1269.51.

[5-(4-Dimethylaminophenylethynyl)-15-(5-nitrothiazol-2-ylethynyl)-10,20-bis(3,5-bis(3,3-dimethyl-1-butyloxy)phenyl)porphinato]zinc(II) (Compound 5). Porphyrin 3 (144 mg, 132 μmol), 2-bromo-5-nitrothiazole (273 mg, 1306 μmol), Pd(PPh₃)₄ (97 mg, 83.9 μmol), CuI (27 mg, 142 μmol), THF (25 mL), and (*i*-Pr)₂NEt (2 mL) were placed in a 100 mL Schlenk tube, and the mixture was heated at 54 °C for 23 h. After cooling to RT, the reaction mixture was poured into a saturated NaCl solution, extracted with CHCl₃, dried over Na₂SO₄, filtered, and evaporated. The brownish-green residue was chromatographed sequentially over silica gel (3:1 hexanes/THF), Bio-Beads SX-1 (THF), and silica gel (19:11 CHCl₃/THF). Yield: 85 mg (53%, based on 144 mg of the porphyrinic starting material). ¹H NMR (CDCl₃/TMS/1-drop-pyridine-*d*₅): δ 9.67 (d, 2 H, β, *J* = 4.51), 9.48 (d, 2 H, β, *J* = 4.53), 8.98 (d, 2 H, β, *J* = 4.56), 8.90 (d, 2 H, β, *J* = 4.58), 8.59 (*br. s.*, 1 H, thiazolic C–H), 7.84 (d, 2 H, Ar, *J* = 8.65), 7.33 (d, 4 H, Ar, *J* = 2.08), 6.90 (t, 2 H, Ar, *J* = 2.08, 2.12), 6.80 (d, 2 H, Ar, *J* = 8.66), 4.22 (t, 8 H, OCH₂CH₂, *J* = 7.32, 7.35), 3.06 (s, 6 H, NMe₂), 1.86 (t, 8 H, OCH₂ CH₂, *J* = 7.33, 7.32), 1.01 (s, 36 H, *tert*-butyl). Vis (λ_{max}(log ε); THF): 458 nm (5.07) and 694 nm (4.75). Fluorescence emission (THF): 712 nm. ESI MS: 1219.54 (M⁺), calcd for C₇₁H₇₇N₇O₆SZn: 1219.49; FAB: 1220.6 (MH⁺), calcd for C₇₁H₇₈N₇O₆SZn: 1220.5.

[5-(2-(*N,N*-Diphenylamino)thiophen-5-yl-ethynyl)-15-(4-nitrophenylethynyl)-10,20-bis(3,5-bis(3,3-dimethyl-1-butyloxy)phenyl)porphinato]zinc(II) (Compound 6). *N*-(5-Iodothiophen-2-yl)-diphenylamine (92 mg, 244 μmol), porphyrin 4 (64 mg, 55.3 μmol), Pd(PPh₃)₄ (64 mg, 55.3 μmol), CuI (19 mg, 99.7 μmol), THF (20 mL), and (*i*-Pr)₂NH (2 mL) were placed in a 100 mL Schlenk tube under nitrogen. The reaction vessel was shielded from light and stirred at 44 °C for 24 h. After cooling to RT, the dark green reaction mixture was poured into deionized water, extracted with CH₂Cl₂, dried over Na₂SO₄, filtered, and evaporated. The green residue was chromatographed sequentially over silica gel (4:1 hexanes/THF), Bio-Beads SX-1 (THF), and silica gel (CHCl₃) to give a green solid. Yield: 22 mg (44%, based on 64 mg of the porphyrinic starting material). ¹H NMR (CDCl₃/TMS/pyridine-*d*₅): δ 9.61 (d, 2 H, β, *J* = 4.68), 9.58 (d, 2 H, β, *J* = 4.67), 8.99 (d, 2 H, β, *J* = 4.68), 8.93 (d, 2 H, β, *J* = 4.68), 8.36 (d, 2 H, Ar, *J* = 8.77), 8.06 (d, 2 H, *J* = 8.83), 7.47 (d, 1 H, *J* = 3.95), 7.40–7.29 (m, 12 H, Ar), 7.14 (m, 2 H, *para*-Ar), 6.89 (t, 2 H, *J* = 2.16, 2.05), 6.70 (d, 1 H, thienyl, *J* = 3.94), 4.20 (t, 8 H, *J* = 7.30, 7.36), 1.85 (t, 8 H, *J* = 7.31, 7.28), 1.01 (s, 36 H, *tert*-butyl). Vis (λ_{max}(log ε); THF): 458 nm (5.02), 674 nm (4.63). Fluorescence emission (THF): 713 nm. MALDI-TOF (MH⁺): 1343.8, calcd for C₈₂H₈₂N₆O₆SZn + H: 1343.5.

[5-(2-(9*H*-Carbazol-9-yl)-thiophen-5-yl-ethynyl)-15-(4-nitrophenylethynyl)-10,20-bis(3,5-bis(3,3-dimethyl-1-butyloxy)phenyl)-

porphinato]zinc(II) (Compound 7). 9-(5-Iodothiophen-2-yl)-9*H*-carbazole (179 mg, 477 μmol), porphyrin 4 (52.5 mg, 47.9 μmol), Pd₂(dba)₃ (36.3 mg, 39.3 μmol), AsPh₃ (87 mg, 284 μmol), THF (20 mL), and (*i*-Pr)₂NH (2 mL) were placed in a 100 mL Schlenk tube under N₂. The reaction mixture was stirred at 60 °C for 6 h. After cooling to RT, the reaction mixture was evaporated to dryness, and the isolated green residue was chromatographed over silica gel using 5:1 hexanes/THF as the eluant. A green solid was isolated and chromatographed on Bio-Beads SX-1 (THF) followed by silica gel (CHCl₃) to give a green solid. Yield: 52 mg (81%, based on 52.5 mg of the porphyrinic starting material). ¹H NMR (CDCl₃/TMS/pyridine-*d*₅): δ 9.66 (t, 4 H, β, *J* = 4.38, 4.46), 9.01 (t, 4 H, β, *J* = 4.53, 4.86), 8.41 (d, 2 H, Ar, *J* = 9.04), 8.16 (d, 2 H, Ar, *J* = 7.84), 8.12 (d, 2 H, Ar, *J* = 8.89), 7.77 (d, 1 H, thienyl, *J* = 3.86), 7.71 (d, 2 H, Ar, *J* = 8.11), 7.53 (m, 2 H, Ar), 7.41–7.32 (m, 7 H, 6 Ar + 1 thienyl), 6.89 (t, 2 H, *J* = 2.17, 2.18), 4.21 (t, 8 H, average *J* = 7.33), 1.83 (t, 8 H, average *J* = 7.30), 1.01 (s, 36 H, *tert*-butyl). Vis (λ_{max}(log ε); THF): 459 nm (5.08) and 665 nm (4.69). Fluorescence emission (THF): 682 nm. MALDI-TOF (M⁺): 1340.73, calcd for C₈₂H₈₀N₆O₆SZn: 1340.52.

Results and Discussion

Design and Synthesis. The syntheses of a series of conjugated (porphinato)zinc(II) (PZn)-based chromophores (Figure 1) structurally related to **compound 1**²⁹ are outlined in Schemes 1 and 2. These porphyrinic compounds exploit arylolethynyl-, thienylethynyl-, thiazolylolethynyl-, benzothiazolylolethynyl-, and carbazolylolethynyl-based donor (D) and acceptor (A) moieties. Note that two structures (**compounds 6** and **7**) feature 4-nitrophenylethynyl electron-withdrawing moieties, while **compounds 1–5** define a set of chromophores having a fixed 4-dimethylaminophenylethynyl electron-releasing group.

All of these chromophores derive from a common synthon^{26,29} (**porphyrin 1**, see Experimental Section) and a succession of metal-catalyzed cross-coupling reactions.³⁸ Fabrication of **compounds 1–7** proceeds through the intermediacy of either brominated **porphyrin 2**²³ (see Experimental Section) or ethynylated **porphyrin 4**^{26,29} (see Experimental Section) intermediates and appropriately functionalized aryl, thienyl, thiazolyl, benzothiazolyl, and carbazolyl reagents. **Compounds 1–7** all feature a 5,15-diethynyl(porphinato)zinc(II) core, a structural motif well established as a key component of a wide range of potent NLO chromophores.^{23,26,28,29,31,42,43}

Figure 2 emphasizes the various conjugated, π aromatic components of **compounds 1–7**. Previous studies establish that enhanced hyperpolarizabilities in classic NLO push–pull chromophore structures based on aryl donor, bridge, and acceptor components are often observed upon heteroaromatic replacement of these units, as such species possess typically a lower aromatic stabilization (delocalization) energy (Supporting Information);^{1,2,7,10,19–21,29,44,45} PZn-based structures

(42) Priyadarshy, S.; Therien, M. J.; Beratan, D. N. *J. Am. Chem. Soc.* **1996**, *118*, 1504–1510.

(43) Karki, L.; Vance, F. W.; Hupp, J. T.; LeCours, S. M.; Therien, M. J. *J. Am. Chem. Soc.* **1998**, *120*, 2606–2611.

(44) Waite, J.; Papadopoulos, M. G. *J. Phys. Chem.* **1990**, *94*, 6244–6249.

(45) Hsu, C.-C.; Shu, C.-F.; Huang, T.-H.; Wang, C. H.; Lin, J.-L.; Wang, Y.-K.; Zang, Y.-L. *Chem. Phys. Lett.* **1997**, *274*, 466–472.

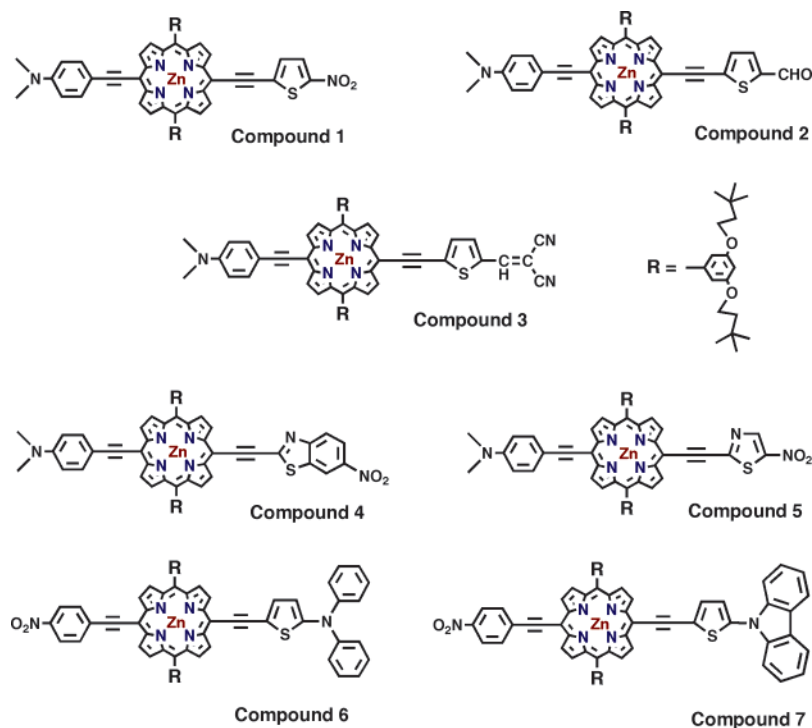
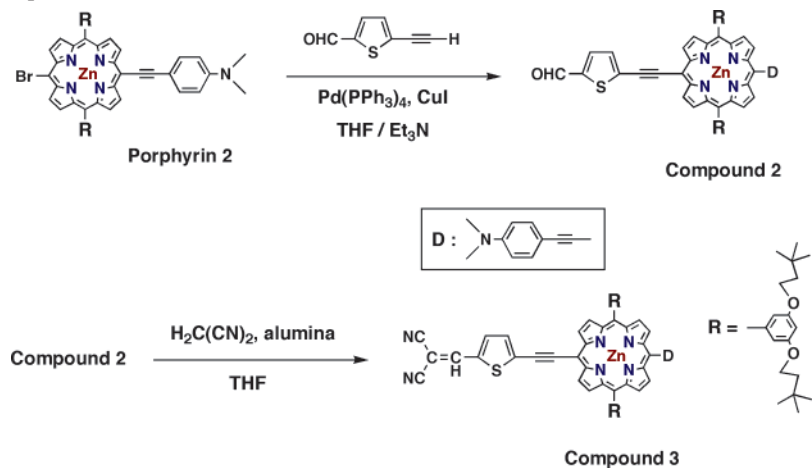


Figure 1. Structures of the push-pull (hetero)arylethynyl porphyrins investigated.

Scheme 1. Syntheses of Compounds 2 and 3



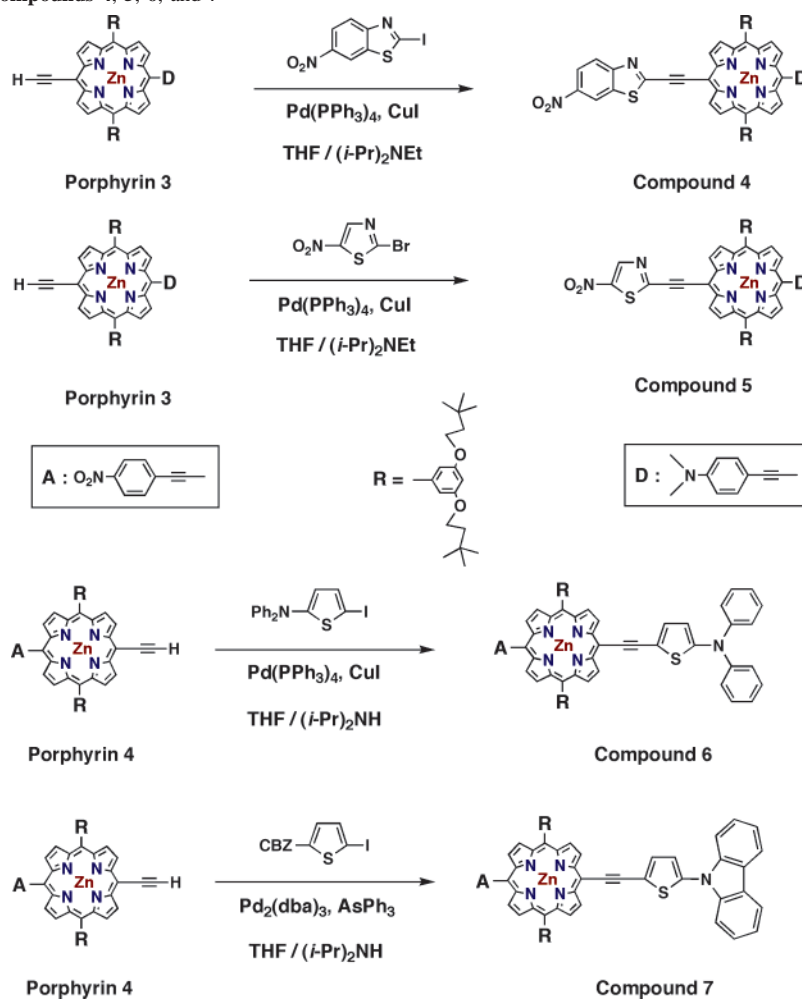
1–7 thus differ from the archetypal push-pull [bis(aryl-ethynyl)porphyrinato]zinc(II) NLO chromophore^{23,42} and exploit ethynylthiophene, ethynylthiazole, and ethynylbenzothiazole components. Motivating factors for selection of diphenylamino-*N*-thiophen-2-yl-5-ethynyl,^{11,46–50} 5-(carbazol-9-yl-thiophen-2-yl-5-ethynyl,^{51–55} 2-formyl-thiophen-5-yl-ethynyl, 2-(2,2-dicyanovinyl)-thiophen-5-yl-ethynyl,^{2,9,10,56–58} and 6-nitro-benzothiazol-2-yl-ethynyl^{3,4} electron-releasing

and electron-withdrawing components in 1–7 are congruent with established literature precedent; the Supporting Information correlates the lower aromatic stabilization energy of these heteroaromatic electron-releasing and -withdrawing units with a substantial body of spectroscopic data.

- (46) Moylan, C. R.; Twieg, R. J.; Lee, V. Y.; Swanson, S. A.; Bettegton, K. M.; Miller, R. D. *J. Am. Chem. Soc.* **1993**, *115*, 12599–12600.
 (47) Verbiest, T.; Burland, D. M.; Jurich, M. C.; Lee, V. Y.; Miller, R. D.; Volksen, M. *Science* **1995**, *268*, 1604–1606.
 (48) Whitaker, C. M.; Patterson, E. V.; Kott, K. L.; McMahon, R. J. *J. Am. Chem. Soc.* **1996**, *118*, 9966–9973.
 (49) Thayumanavan, S.; Barlow, S.; Marder, S. R. *Chem. Mater.* **1997**, *9*, 3231–3235.
 (50) Yang, J.-S.; Chiou, S.-Y.; Liau, K.-L. *J. Am. Chem. Soc.* **2002**, *124*, 2518–2527.

- (51) Zhang, Y.-D.; Wang, L.; Wada, T.; Sasabe, H. *Chem. Commun.* **1996**, 559–561.
 (52) Zhang, Y.-D.; Wang, L.; Wada, T.; Sasabe, H. *Macromolecules* **1996**, *29*, 1569–1573.
 (53) Zhang, Y.; Wada, T.; Sasabe, H. *J. Mater. Chem.* **1998**, *8*, 809–828.
 (54) Meshulam, G.; Berkovic, G.; Kotler, Z.; Ben-Asuly, A.; Mazor, R.; Shapiro, L.; Khodorkovsky, V. *Synth. Met.* **2000**, *115*, 219–223.
 (55) Meshulam, G.; Berkovic, G.; Kotler, Z. *Opt. Lett.* **2001**, *26*, 30–32.
 (56) Katz, H. E.; Singer, K. D.; Sohn, J. E.; Dirk, C. W.; King, L. A.; Gordon, H. M. *J. Am. Chem. Soc.* **1987**, *109*, 6561–6563.
 (57) Kuder, J. E.; Limburg, W. W.; Pochan, J. M.; Wychick, D. *J. Chem. Soc., Perkin 2* **1977**, 1643–1651.
 (58) Wu, X. M.; Wu, J.; Liu, Y.; Jen, A. K. Y. *Chem. Commun.* **1999**, 2391–2392.

Scheme 2. Syntheses of Compounds 4, 5, 6, and 7



Linear and Nonlinear Optical Properties. For these dipolar molecules, the diagonal component β_{zzz} of the molecular first hyperpolarizability (or second-order nonlinear polarizability) tensor has been evaluated (see Experimental Section). The molecular first hyperpolarizability, β , was determined by HRS measurements for **compounds 1–7** in THF solution.^{59,60} As these compounds fluoresce, it is essential to use a femtosecond (fs) pulsed laser in these experiments in order to discriminate between scattering (immediate and hyper-Rayleigh) and time-delayed, multiphoton fluorescence. Our approach for eliminating a multiphoton contribution to the HRS signal involves a Fourier transform of the

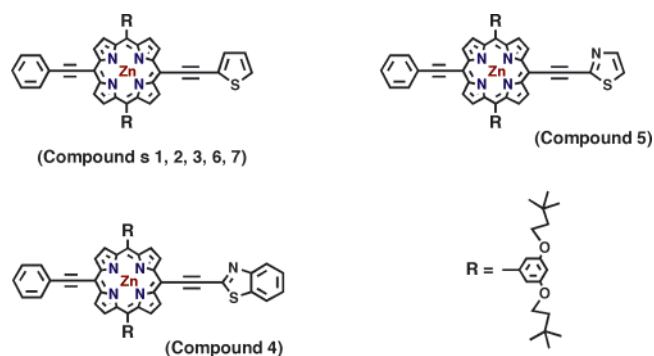


Figure 2. Conjugated, π aromatic frameworks to which antipodal electron-releasing and electron-withdrawing groups are attached in **compounds 1–7**.

frequency domain data to the time domain: as the fluorescence is to a large extent delayed in time, it is advantageous to measure the HRS signal at early times following the incident fundamental laser pulse.⁶¹ In the frequency domain, this results in any fluorescence signals being phase-shifted and diminished in amplitude with increasing amplitude modulation (AM) frequencies.^{62,63} Such fs HRS measurements of fluorescent molecules that discriminate between scattering and multiphoton fluorescence are performed at successively higher AM frequencies. The analysis of the frequency-dependent apparent hyperpolarizability data provides a true (fluorescence-free) hyperpolarizability value at infinitely high frequency, the magnitude of the multiphoton fluorescence contribution at zero frequency, and a fluorescence lifetime; this latter quantity can be compared with the corresponding fluorescence lifetime obtained from time-correlated single-photon counting (TCSPC) experiments.

To verify temporal, thermal, and photochemical stability of chromophores **1–7** under these HRS nonlinear optical

(59) Clays, K.; Persoons, A. *Phys. Rev. Lett.* **1991**, *66*, 2980–2983.

(60) Clays, K.; Persoons, A. *Rev. Sci. Instrum.* **1992**, *63*, 3285–3289.

(61) Noordman, O. F. J.; van Hulst, N. F. *Chem. Phys. Lett.* **1996**, *253*, 145–150.

(62) Olbrechts, G.; Strobbe, R.; Clays, K.; Persoons, A. *Rev. Sci. Instrum.* **1998**, *69*, 2233–2241.

(63) Wostyn, K.; Binnemans, K.; Clays, K.; Persoons, A. *Rev. Sci. Instrum.* **2001**, *72*, 3215–3220.

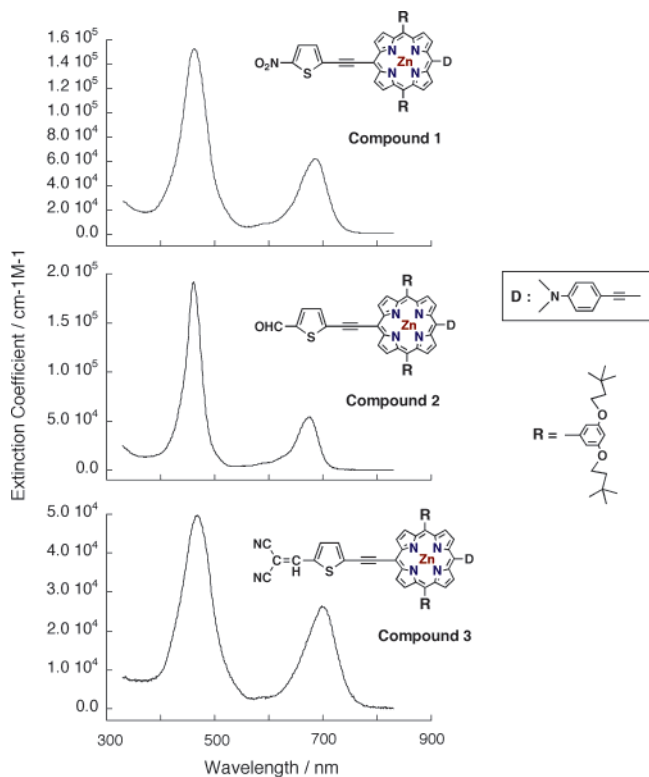


Figure 3. Comparative ground-state electronic absorption spectra for **compounds 1, 2, and 3** in THF solvent.

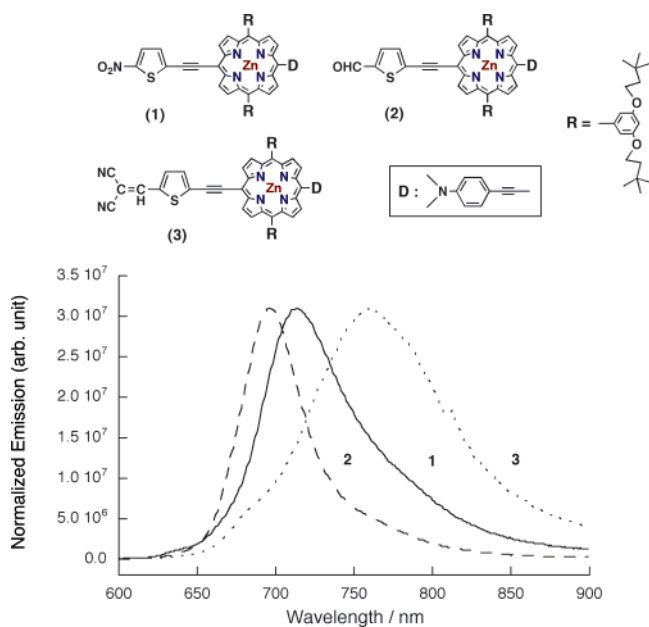


Figure 4. Comparative fluorescence emission spectra for **compounds 1, 2, and 3** in THF solvent.

measurement conditions (high peak power pulsed illumination over multiple measurement cycles), electronic absorption and emission spectra (Figures 3–8) were compared before and after acquisition of NLO data; these studies indicated that all these species were robust. The apparent dynamic hyperpolarizability as a function of modulation frequency for **1–7** did show an appreciable frequency dependence and phase accumulation for increasing modulation frequencies at 1300 nm. Therefore, the dynamic apparent hyperpolarizability values at this wavelength were extrapolated to the

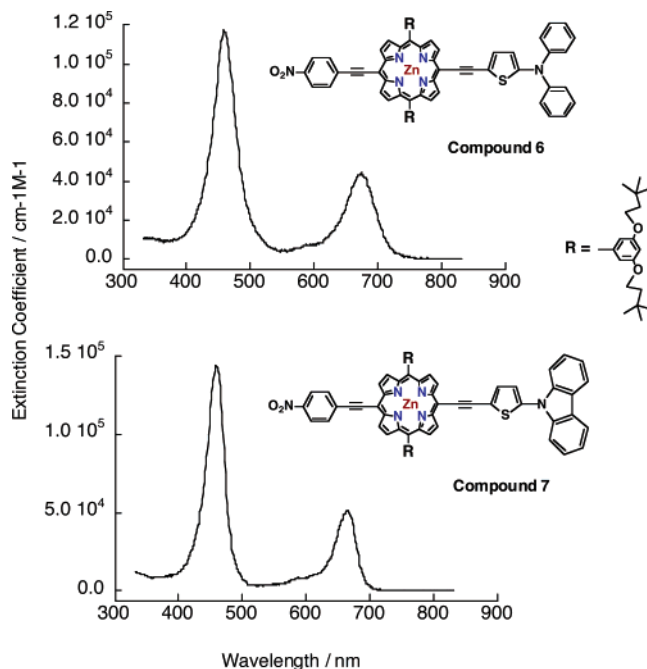


Figure 5. Comparative ground-state electronic absorption spectra for **compounds 6 and 7** in THF solvent.

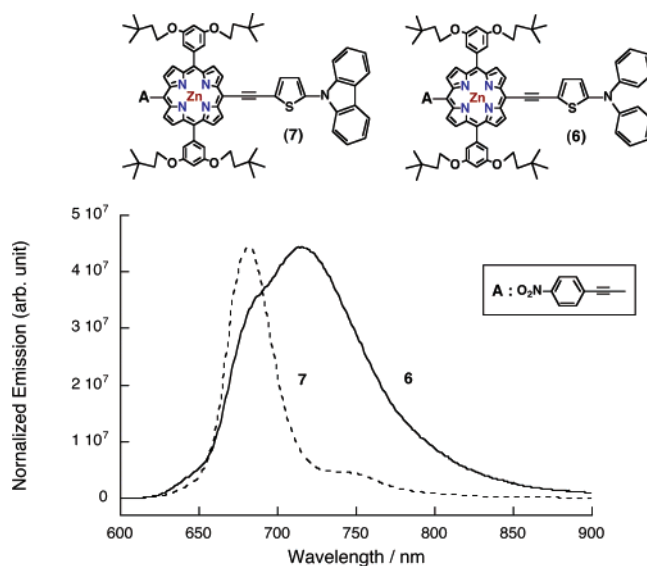


Figure 6. Comparative fluorescence emission spectra for **compounds 6 and 7** in THF solvent.

high-frequency limit; simultaneous fitting of the amplitude and the phase data determines the fluorescence-free first hyperpolarizability value (Figure 9). Table 1 provides an overview of the linear and nonlinear optical properties of this series of chromophores.

The **compound 1** benchmark,²⁹ which features dimethylaminophenylethynyl-donor and nitrothiophenylethynyl-acceptor moieties, shows a sizable dynamic hyperpolarizability at 1300 nm (690×10^{-30} esu). An important factor governing the magnitude of the dynamic hyperpolarizability value in oligothiophenyl and oligothiophenylethynyl elaborated porphyrin-based chromophores has been shown to be the degree of Q-state derived resonance enhancement factor. For these compounds, this value is largely determined by the proximity of the *x*-polarized⁴¹ Q-band λ_{max} value to the second harmonic

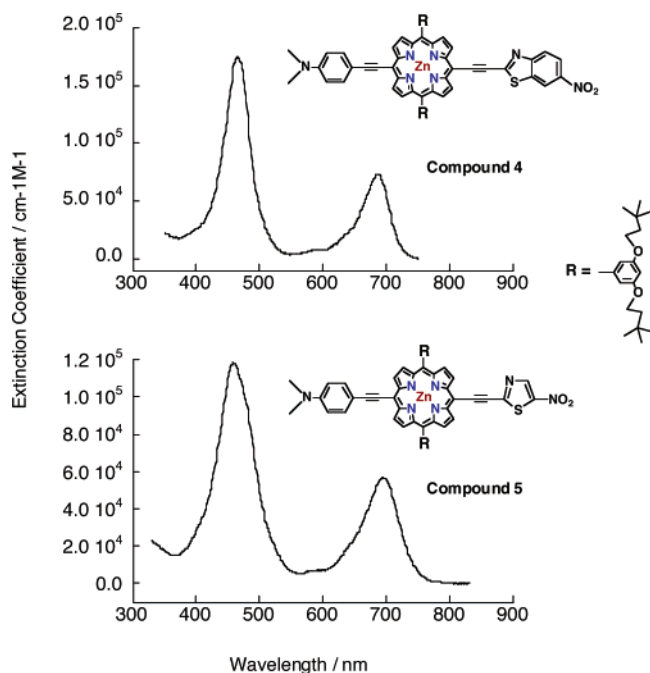


Figure 7. Comparative ground-state electronic absorption spectra for **compounds 4 and 5** in THF solvent.

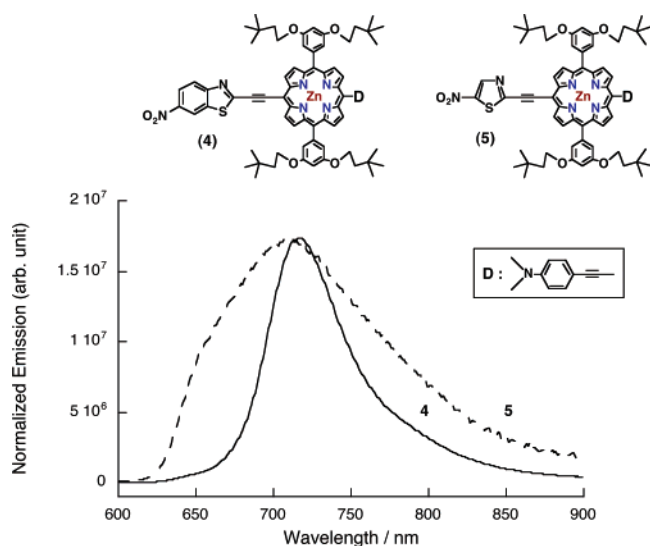


Figure 8. Comparative fluorescence emission spectra for **compounds 4 and 5** in THF solvent.

wavelength of 650 nm, when performing HRS experiments at 1300 nm.²⁹ The impact of 2-photon resonance enhancement can be appreciated within the context of a simple 2-level formulation of β (eq 1).^{64–66}

$$\beta'_n = \frac{6(P_{ge})_n^2(\Delta\mu_{ge})_n(E_{op})_n^2}{[(E_{op})_n^2 - (2E_{inc})^2][(E_{op})_n^2 - E_{inc}^2]} \quad (1)$$

In the above equation, E_{op} is the energy of the optical transition of interest, and P_{ge} and $\Delta\mu_{ge}$ are, respectively, the transition strength and ground-to-excited-state dipole moment change associated with the charge-transfer absorption.

(64) Oudar, J. L.; Chemla, D. S. *J. Chem. Phys.* **1977**, *66*, 2664–2668.

(65) Oudar, J. L. *J. Chem. Phys.* **1977**, *67*, 446–457.

(66) Willetts, A.; Rice, J. E.; Burland, D. M.; Shelton, D. P. *J. Chem. Phys.* **1992**, *97*, 7590–7599.

Compounds 2 and 3, which possess, respectively, formyl and dicyanovinyl acceptor groups,^{31,56} confirm these earlier conclusions. Previous studies examining hyperpolarizable porphyrin-based donor–acceptor chromophores that feature thiophenyl, [2,2']bithiophenyl, and [2,2';5',2'']terthiophenyl units terminated with a 5-nitro group and points of connectivity that vary between the macrocycle meso-carbon position and meso-appended-ethynyl moiety show that the spectral position of the x -polarized Q-state derived absorption maximum and, hence, the first hyperpolarizability value are dependent upon the number of intervening thiophene units. The Table 1 data show that modulation of the thieryl acceptor strength (Supporting Information) at constant conjugation length controls similarly the Q-band λ_{max} value. Because the Soret (B band) absorption λ_{max} value lies far from the λ_{inc} second-harmonic wavelength (650 nm) and varies little in **compounds 1–7**, the resonance enhancement originating from the B-state manifold centered near 450 nm can be considered near constant. As the Q-band absorption λ_{max} is sensitive to the nature of the acceptor in **1–3**, electronic modulation at the thieryl 2-position has a pronounced effect on measured dynamic first hyperpolarizabilities. Because **compound 2**'s formyl group drives a blue-shift of the Q-band λ_{max} toward the second-harmonic wavelength relative to that observed for **compound 1**, while the stronger dicyanovinyl acceptor in **compound 3** effects a corresponding x -polarized Q-state red-shift, **compound 2** possesses the largest β_{1300} value of these three chromophores. Note that the impact of decreasing the $E_{op} - 2E_{inc}$ energy separation in this spectral region (**compound 2**) has a much greater impact on the magnitude of β_λ than does the augmentation of P_{ge} and $\Delta\mu_{ge}$ (eq 1) that derives from the superior dicyanovinyl acceptor (**compound 3**; see Figure 3, Table 1).

With respect to the linear spectroscopy of these compounds, it is clear that the relative acceptor strength is also reflected in the fluorescence Stokes shift. The Stokes shifts for **compounds 1–7** vary from 364 to 1150 cm^{-1} , indicating that these PZn-based chromophores undergo modest-to-substantial excited-state electronic structural redistributions. These Stokes shift data are consistent with expectations based on (i) previous studies of closely related D–A derivatized PZn chromophores,^{9,38,42,67,68} (ii) electronic structural effects arising from the integration of heteroaromatics possessing modest aromatic stabilization energies along molecular axis of highest conjugation,^{13,30,68–71} and (iii) the energetic proximity of the D, PZn-based bridge, and A frontier orbital energy levels,^{9,30,38,42,67,68} which suggest that the excited states of these species should possess an appreciable quinoidal

(67) Garcia, P.; Pernaut, J. M.; Hapiot, P.; Wintgens, V.; Valat, P.; Garnier, F.; Delabouglise, D. *J. Phys. Chem.* **1993**, *97*, 513–516.

(68) Rao, V. P.; Cai, Y. M.; Jen, A. K. Y. *Chem. Commun.* **1994**, 1689–1690.

(69) Chosrovian, H.; Rentsch, S.; Grebner, D.; Dahm, D. U.; Birckner, E.; Naarmann, H. *Synth. Met.* **1993**, *60*, 23–26.

(70) Becker, R. S.; de Melo, J. S.; Macanita, A. L.; Elisei, F. *J. Phys. Chem.* **1996**, *100*, 18683–18695.

(71) Pappenfus, T. M.; Raff, J. D.; Hukkanen, E. J.; Burney, J. R.; Casado, J.; Drew, S. M.; Miller, L. L.; Mann, K. R. *J. Org. Chem.* **2002**, *67*, 6015–6024.

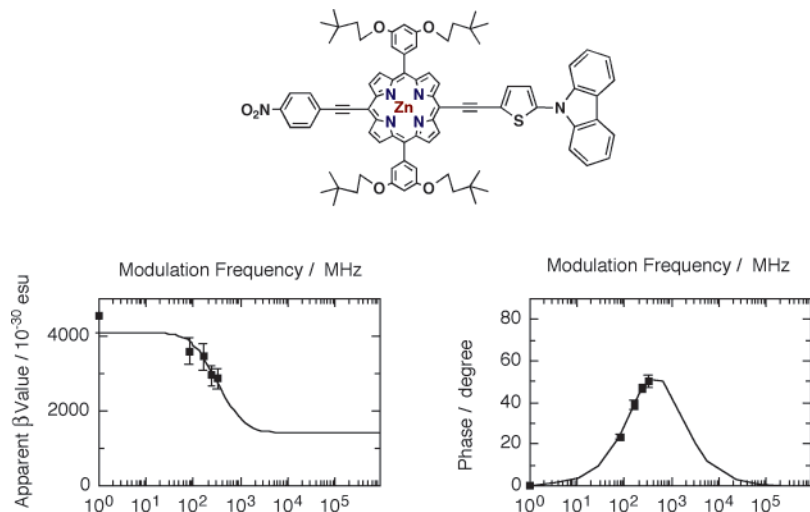


Figure 9. Typical dependence of measured values, and the phase angle between the HRS signal and fluorescence reference signal, determined as a function of modulation frequency. Data displayed are for **compound 7**.

Table 1. Linear and Nonlinear Optical Properties for Porphyrin Chromophores **1–7** in THF Solvent

chromophore	B band $\lambda_{\max}/(\text{nm})$	Q-band $\lambda_{\max}/(\text{nm})$	fluorescence $\lambda_{\text{em}}/(\text{nm})$	$E_{0,0}$ (eV)	Stokes shift (cm^{-1})	β_{1300} (10^{-30} esu)
1	465	685	714	2.16	593	690
2	461	676	696	2.18	425	1020
3	469	698	759	2.12	1151	785
4	465	686	716	2.15	611	1140
5	458	694	712	2.15	364	1000
6	458	674	713	2.19	812	810
7	459	665	682	2.20	375	1400

resonance contribution. The quinoidal resonance form enhances the extent to which electron density is redistributed between the electron-releasing and electron-accepting components of these chromophores in the excited state. Consistent with the large dicyanovinyl acceptor strength, **compound 3** possesses the largest magnitude Stokes shift and the lowest energy fluorescence emission λ_{\max} . Note that, while the Stokes shift reflects the extent of ground-to-excited-state electronic charge redistribution ($\Delta\mu_{\text{ge}}$) and has been often taken as a qualitative measure of chromophoric static hyperpolarizability, the fact that these values do not track with the experimentally determined dynamic hyperpolarizabilities (Table 1), points to the over-riding importance of Q-state derived resonance enhancement factor in determining the β_{1300} value for **compounds 1–7**.

Compounds 6 and 7 are **compound 1** analogues in which the charge-transfer direction is inverted; note that in **6** and **7** that it is the aryl ring that bears the 4'-nitro group while the thienyl unit features a 2'-electron-releasing moiety. This electronic structural modification has only a modest impact upon the electronic absorption spectra of these species relative to that of the **compound 1** benchmark (Figures 3 and 5, Table 1); in contrast, the emission spectra of these species (Figures 4 and 6) reflect that diminished excited-state structural heterogeneity is manifest in **compound 7** relative to **compounds 1** and **6**, which derives from the fact that the **compound 7** electron-releasing group is a planar, conjugated carbazolyl unit. Note that the *x*-polarized Q-state absorption of **6** and **7** are blue-shifted relative to **compound 1**; hence, the measured dynamic hyperpolarizability values at $\lambda_{\text{inc}} = 1300$ nm are affected by resonance enhancement

in much the same way as discussed above for **compounds 1–3** (Table 1). While **compound 6** and **7** β_{1300} values exceed that measured for **compound 1**, note that the observed enhancement in nonlinear response determined in **7** exceeds that of **compounds 1** and **6** by approximately 2-fold.

For **compound 1–7**, it is noteworthy that oscillator strengths of the low energy Q-state electronic manifolds are virtually identical (Figures 3, 5, and 7). Considering **compounds 6** and **7** as a case in point (Figure 5), it is clear that a diminished $S_0 \rightarrow S_1$ transition energy is not correlated with an increase in the first hyperpolarizability. Reductions in the magnitude of the optical band gap, however, are commonly correlated with augmented first hyperpolarizabilities; this effect is commonly referred to as the nonlinearity/transparency tradeoff.^{72,73} That this correlation is not observed in **6** and **7** and throughout the range of chromophores described herein derives likely from the transfer of oscillator strength between overlapping $\pi-\pi^*$ and CT transitions within the low-energy transition manifold as a function of the nature of electron-releasing and electron-withdrawing components in these structures. This effect has been noted in closely related chromophores.²⁹ Hence, as highlighted in Figure 5 (see also Figures 3 and 7), P_{ge} remains relatively constant while $\Delta\mu_{\text{ge}}$ varies with nature of donor and acceptor; small reductions in the $E_{\text{op}} - 2E_{\text{inc}}$ energy gap thus enable large modulations in the β_{1300} value in **compounds 1–7** at approximately constant chromophoric transparency.

(72) Ledoux, I.; Zyss, J.; Jutand, A.; Amatore, C. *Chem. Phys.* **1991**, *150*, 117–123.

(73) Cheng, L.-T.; Tam, W.; Stevenson, S. H.; Meredith, G. R.; Rikken, G.; Marder, S. R. *J. Phys. Chem.* **1991**, *95*, 10631–10643.

Compounds 4 and **5** probe the effect of diminishing the acceptor aromatic stabilization energy (Supporting Information) relative to the **compound 1** benchmark. **Compounds 4** and **5** utilize, respectively, nitrobenzothiazolyethynyl and nitrothiazolyethynyl acceptor groups and a dimethylaminophenylethynyl donor unit in common with **compound 1**. As seen in the linear absorption spectra (Figure 7), the reduced acceptor aromatic stabilization energies in **6** and **7** effect a similar spectroscopic perturbation relative to the **compound 1** spectrum, as was observed when the dicyanovinyl unit was introduced to the thienyl 2-position (**compound 3**, Figure 3). Consistent with the above discussion, differences in the measured dynamic hyperpolarizabilities of **compounds 3**, **4**, and **5** track qualitatively with the extent of Q-state derived resonance enhancement (Table 1).

Conclusion

A series of conjugated (porphinato)zinc(II)-based chromophores structurally related to **compound 1**²⁹ were synthesized using metal-catalyzed cross-coupling reactions involving [5-bromo-15-triisopropylsilylethynyl-10,20-diarylporphinato]zinc(II), [5-bromo-15-(4-dimethylaminophenylethynyl)-10,20-diarylporphinato]zinc(II), [5-(4-dimethylaminophenylethynyl)-15-ethynyl-10,20-diarylporphinato]zinc(II), and [5-(4-nitrophenylethynyl)-15-ethynyl-10,20-diarylporphinato]zinc(II), with appropriately functionalized aryl, thienyl, thiazolyl, benzothiazolyl, and carbazolyl precursors. The measured β_{1300} values for these hyperpolarizable (porphinato)zinc(II) chromophores that feature ethynylthiophenyl-, ethynylthiazolyl-, and ethynylbenzothiazolyl-based electron-releasing and -withdrawing groups ranged from 690 \rightarrow 1400 $\times 10^{-30}$ esu and highlight the extent to

which reductions in the magnitude of the aromatic stabilization energy of these groups impact the molecular hyperpolarizability.

Recent studies examining hyperpolarizable porphyrin-based donor–acceptor chromophores that feature thiophenyl, [2,2']bithiophenyl, and [2,2';5',2'']terthiophenyl units terminated with a 5-nitro group, and points of connectivity that vary between the macrocycle meso-carbon position and meso-appended-ethynyl moiety, show that β_{1300} values as large as 4350 $\times 10^{-30}$ esu can be engineered.²⁹ The fact that this work demonstrates that classic donor–acceptor electronic modulation of the **compound 1** benchmark ($\beta_{1300} = 690 \times 10^{-30}$ esu) leads to significantly enhanced hyperpolarizabilities, suggests that further improvements in the already large magnitude β_{1300} values expressed within this broader family of porphyrin-oligo(aromatic heterocycle)-based neutral dipolar chromophores should be possible.

Acknowledgment. This work was funded through grants from the Office of Naval Research N00014-01-1-0725, the U. S. Department of Energy (DE-FG02-04ER46156), the Belgian government (IUAP/5/3), the Flemish Fund for Scientific Research (G.0261.04), and the University of Leuven (G0A/2000/03). M.J.T. thanks the MRSEC Program of the National Science Foundation (DMR00-79909) for infrastructural support.

Supporting Information Available: Syntheses and characterization data for key precursor structures and chromophoric benchmarks; Hammett correlation analysis, NMR, absorption, and emission data for porphyrin-based compounds. This material is available free of charge via the Internet at <http://pubs.acs.org>.

IC060898E